Elastic scattering of ^{6}He from ^{12}C at 38.3 MeV/nucleon*

DONG Hong-Fei(董鸿飞)[1,2] MA Yin-Qun(马引群)[1,3;1)] MA Zhong-Yu(马中玉)[3]

1 (Department of Physics, Taiyuan Normal University, Taiyuan 030031, China)
2 (Department of Physics, Chifeng College, Chifeng 024001, China)
3 (China Institute of Atomic Energy, Beijing 102413, China)

Abstract The microscopic optical potential of nucleus-nucleus interaction is presented via a folding method with the isospin dependent complex nucleon-nuclear potential, which is first calculated in the framework of the Dirac-Bruecker-Hartree-Fock approach. The elastic scattering data of ^{6}He at 229.8 MeV on ^{12}C target are analyzed within the standard optical model. To take account of the breakup effect of ^{6}He in the reaction an enhancing factor 3 on the imaginary potential is introduced. The calculated ^{6}He+^{12}C elastic scattering differential cross section is in good agreement with the experimental data. Comparisons with results in the double-folded model based on the M3Y nucleon-nucleon effective interaction and the few the body Glauber-model calculations are discussed. Our parameter free model should be of value in the description of nucleus-nucleus scattering, especially unstable nucleus-nucleus systems.

Key words microscopic optical potential, Dirac-Bruecker-Hartree-Fock approach, folding model, nucleus-nucleus elastic scattering

PACS 24.10.Jv, 21.65.+f, 25.55.Ci

1 Introduction

The nucleus-nucleus potential is a quantity of importance not only for the description of elastic cross sections but also as an ingredient in the description of all the phenomena which occur when two nuclei collide[1]. The study of a nucleus-nucleus optical potential is one of the fundamental subjects in nuclear physics. In particular, it is very important to understand the complex optical potential for composite projectiles from a microscopic point of view not only to understand the relevant reaction dynamics involved but also to develop a practical tool for predicting optical potentials of colliding systems for which the elastic scattering measurement is absent or difficult, such as in the case of neutron-rich or proton-rich β-unstable nuclei. In those cases the elastic scattering can be strongly affected by reaction channels, which are strongly connected to the elastic channel, such as collective excitation channels of deformed nuclei or projectile breakup channels of loosely bound systems. There exists a strong dynamic polarization effect that has to be accounted for, that is, coupled-channel (CC) calculations. In such cases, a microscopic interaction model serves as a tool for providing the "bare" optical potential to be used in CC calculations, rather than the net optical potential which includes dynamic polarization effects[2].

A fully microscopic calculation of the nucleus-nucleus interaction is quite complicated. One of the simplest and most practical tools for constructing the microscopic optical potential between complex nuclei is the double folding model (DFM). In the DFM, an effective nucleon-nucleon (NN) interaction in the nuclear medium is doubly folded with nucleon density distributions in projectile and target nuclei. One of the most successful effective NN interactions is the so-called M3Y $\boldsymbol{G}$-matrix interaction[3] or its density-dependent version, CDM3Y6[4]. The DFM with the CDM3Y6 interaction, however, provides us only with the real part of the nucleus-nucleus potential. An imaginary potential must be added to the real DFM

Received 21 October 2008

* Supported by National Natural Science Foundation of China (10475116, 10535010, 10235030) and National Basic Research Program of China (2007cb815000)

1) E-mail: myqfal@ciae.ac.cn

potential by hand. The imaginary potential is normally assumed to have some suitable functional form[5, 6], such as a Woods-Saxon form or its derivative, and the potential parameters included are determined phenomenologically so as to reproduce the experimental data of the elastic scattering. In the past DFM[1, 7, 8] has been widely used to generate the real part of nucleus-nucleus optical potentials, while the imaginary part of the optical potentials remains phenomenological.

2 Theoretical framework

Recently a relativistic microscopic optical potential of a nucleon scattering off a nucleus has been investigated within the framework of the Dirac-Brueckner-Hartree-Fock (DBHF) approach[9]. A new decomposition of the Dirac structure of nuclear self-energy in the DBHF approach was extended to the calculations in asymmetric nuclear matter. The real part of the nucleon self-energy in asymmetric nuclear matter is calculated with the $\boldsymbol{G}$-matrix in the Hartree-Fock approach and the imaginary part of the nucleon self-energy is obtained by the $\boldsymbol{G}$-matrix polarization diagram. The nucleon-nucleus optical potentials in finite nuclei are related to the self-energy of nucleon in nuclear matter by means of the local density approximation (LDA), in which the space distribution of the optical potential is directly connected with the density and asymmetry parameters of the nuclear self-energies in the asymmetric nuclear matter. Nucleon scattering off a nucleus was analyzed with a Schrödinger-type equation, which was obtained by eliminating the lower component of the Dirac spinor in the Dirac equation. A satisfactory agreement with experimental data was found. Encouraged by the success of the isospin-dependent optical potentials in the DBHF approach for nucleon-nucleus scattering[9], we apply this scheme to investigate nucleus-nucleus scattering by a folding method in this letter. Considering the target as just a scatterer, one takes the nucleon-target scattering as an elementary ingredient. The real and imaginary parts of the nucleus-nucleus optical potential are obtained by folding the Schrödinger equivalent potentials of proton- and neutron-nucleus scattering with the density distribution of protons and neutrons in the projectile.

Before we set the stage for the analysis of nucleus-nucleus elastic scattering data, we give a brief description of our theoretical model. Starting from a bare NN interaction V, which is fitted to NN scattering phase shifts and deuteron ground state properties, the NN effective interaction in the nuclear medium is calculated by summing up all ladder diagrams in the DBHF approach. The DBHF $\boldsymbol{G}$ can be decomposed into the bare NN interaction and a correlation term: $\boldsymbol{G} = V + \Delta G$[10]. The correlation term is parameterized by four vertices: scalar, vector and isoscalar, isovector. Due to the characteristic of the short range correlation, they can be described by infinite masses and finite ratios of strengths to the corresponding masses. The nucleon self-energies in nuclear matter are calculated with V and ΔG in the relativistic Hartree-Fock approach. The exchange term produces weak energy dependence of the nucleon self-energy, which takes account of the antisymmetry of the nucleon with all nucleons in the nuclear medium. This is also responsible for a proper isospin dependence of the nucleon effective mass. The DBHF nucleon self-energy in asymmetric nuclear matter has the general form

$$\Sigma^i(k,k_{\rm F},\beta) = \Sigma^i_{\rm s}(k,k_{\rm F},\beta) - \gamma_0\Sigma^i_0(k,k_{\rm F},\beta) + \gamma\cdot\boldsymbol{k}\Sigma^i_v(k,k_{\rm F},\beta)\ , \quad (1)$$

where i stands for proton or neutron. $\beta = (\rho_{\rm n} - \rho_{\rm p})/(\rho_{\rm n} + \rho_{\rm p})$, $\rho_{\rm n}$, $\rho_{\rm p}$ are the asymmetry parameter, neutron and proton densities, respectively. On account of the isovector meson exchanges, the proton and neutron self-energies are distinguishable. The imaginary part of the nucleon self-energy can be obtained by the $\boldsymbol{G}$-matrix polarization diagram. An effective nucleon interaction was introduced in order to avoid the difficulties caused by π-meson and simplify the calculation[9]. Four scalar and vector mesons with density-dependent coupling constants were introduced to reproduce the saturation curves and nucleon self-energies at various densities and asymmetry parameters calculated with the DBHF $\boldsymbol{G}$-matrix.

It is well known that the optical potential of a nucleon in the nuclear medium is equivalent to its self-energy[11—15]. For finite nuclei the nucleon potential is obtained by means of the LDA, in which the space dependence of the relativistic microscopic optical potential (RMOP) is directly connected with the density of the target nucleus and asymmetry parameter in asymmetric nuclear matter:

$$\Sigma_{\rm LDA}(r,\varepsilon) = \Sigma_{\rm NM}[k,\rho(r),\beta], \quad (2)$$

where $\Sigma_{\rm LDA}(r,\varepsilon)$ is the RMOP of a nucleon with an incident energy ε scattering off a finite nucleus, and $\Sigma_{\rm NM}$ is that in nuclear matter at the density ρ and asymmetry parameter β. The Dirac equation of the projectile nucleon in the mean field of the target nu-

cleus can be written as

$$[\boldsymbol{\alpha}\cdot\boldsymbol{k}+\gamma_0(M+U_{\rm s}^i)+U_0^i+V_{\rm C}]\psi^i=E\psi^i\,, \qquad (3)$$

where

$$U_{\rm s}^i=\frac{\Sigma_{\rm s}^i-M\Sigma_{\rm v}^i}{1+\Sigma_{\rm v}^i}, \quad U_0^i=\frac{-\Sigma_0^i+E\Sigma_{\rm v}^i}{1+\Sigma_{\rm v}^i}. \qquad (4)$$

In these expressions, M is the nucleons mass, $U_{\rm s}^i$, U_0^i are Lorentz scalar potential and time like component of a four-vector potential, respectively. $E=\varepsilon+M$, and ε is the energy of the projectile in the center-of-mass system. $V_{\rm C}$ is the Coulomb potential.

In order to calculate the experimental observables, a Schrödinger-equivalent equation for the upper component of the Dirac spinor can be obtained by eliminating the lower component of the Dirac spinor in a standard way[9, 11, 16].

$$\left[\frac{p^2}{2E}+V_{\rm eff}^i(r)+V_{\rm C}(r)+V_{\rm so}^i(r)\boldsymbol{\sigma}\cdot\boldsymbol{L}\right]\Phi^i(\boldsymbol{r})=\frac{E^2-M^2}{2E}\Phi^i(\boldsymbol{r}), \qquad (5)$$

where $V_{\rm eff}^i$ and $V_{\rm so}^i$ are the central and spin-orbit part of the Schrödinger-equivalent potential, respectively, which are known as the nucleon-nucleus optical potential in the non-relativistic approach. The explicit expressions for $V_{\rm eff}^i$ and $V_{\rm so}^i$ are

$$V_{\rm eff}^i=\frac{M}{E}U_{\rm s}^i+U_0^i+\frac{1}{2E}\left[(U_{\rm s}^i)^2-(U_0^i+V_{\rm C})^2\right]+V_{\rm D}^i\,,$$
$$V_{\rm so}^i=-\frac{1}{2{\rm Er}D^i(r)}\frac{{\rm d}D^i(r)}{{\rm d}r}\,, \qquad (6)$$

where $D^i(r)=M+E+U_{\rm s}^i-U_0^i-V_{\rm C}$ and a small Darwin term $V_{\rm D}^i$ is usually neglected. The Schrödinger equivalent potential yields exactly the same scattering phase shifts as the original relativistic potential in the four-component Dirac equation. Therefore we have obtained the microscopic proton- and neutron-nucleus interaction in the framework of the DBHF approach, which are complex with both real and imaginary parts. On account of the isovector meson exchanges the microscopic optical potential also depends on the neutron and proton density distributions of the target nucleus[9].

In a simple practical approach to deal with a composite particle scattering, one considers the target as just a scatterer, and the nucleus-nucleus optical potential can be obtained by a folding method. The proton- and neutron-nucleus optical potentials are folded with the corresponding proton and neutron density distributions in the projectile.

$$V_{\rm FM}(\boldsymbol{R})=\sum_{i=p,n}\int\rho_i(\boldsymbol{r}_i)V_{\rm eff}^i(\boldsymbol{s}_i){\rm d}\boldsymbol{r}_i\,, \qquad (7)$$

where $\boldsymbol{R}$ is the separation distance between two centers of the colliding nuclei. $\boldsymbol{r}_i$ is the coordinate of the proton (neutron) at the center-of-mass frame of the projectile, while $\boldsymbol{s}_i$ is the vector between the proton (neutron) in the projectile and the center of mass of the target, $\boldsymbol{s}_i=\boldsymbol{R}-\boldsymbol{r}_i$. ρ_i is the density distribution of protons (neutrons) at the projectile.

We turn next to the folding method. First, using the technique of momentum representation developed in Ref. [17], we convert Eq. (7) to an expression in momentum space,

$$V_{\rm FM}(\boldsymbol{R})=\sum_{i=p,n}\int\rho_i(\boldsymbol{k}_i)V_{\rm eff}^i(\boldsymbol{k}_i){\rm e}^{i\boldsymbol{k}\cdot\boldsymbol{R}}{\rm d}\boldsymbol{k}_i\,. \qquad (8)$$

This expression becomes much simpler in a spherical assumption, where the density distributions of projectile ρ_i and potential $V_{\rm eff}^i$ are spherical. The Fourier transformation of those quantities can be calculated in a one-dimension integral,

$$V_{\rm eff}^i(k)=4\pi\int_0^\infty j_0(kr)V_{\rm eff}^i(r)r^2{\rm d}r\,,$$
$$\rho_i(k)=4\pi\int_0^\infty j_0(kr)\rho_i(r)r^2{\rm d}r\,, \qquad (9)$$

where $j_0(kr)$ is the zero-order spherical Bessel function. Numerically one could discretize the momentum space and properly choose the momentum basis functions,

$$k_m=m\pi/R_0, \quad w_m^2=(2\pi)^{-3}k_m^2\Delta k_m=m^2/8R_0^3 \qquad (10)$$

The radius R_0 is selected to coincide with the upper limit imposed on the coordinate space integration in practical calculations. The integral with respect to the momentum k in Eq. (8) becomes a summation of series with a limited number m:

$$V_{\rm FM}(R)=\sum_{i=p,n}\left[4\pi\sum_m w_m^2V_{\rm eff}^i(k_m^2)\rho_i(k_m)j_0(k_mR)\right], \qquad (11)$$

The advantage of this method is that it can reduce numerical effort and be easily extended to deformed and excited states.

With the folding method we can obtain the nucleus-nucleus microscopic optical potential with real and imaginary part, simultaneously. To describe nucleus-nucleus elastic scattering one defines the folded microscopic optical potential as,

$$U_{\rm opt}(\boldsymbol{R})={\rm Re}V_{\rm FM}(\boldsymbol{R})+i{\rm Im}V_{\rm FM}(\boldsymbol{R}), \qquad (12)$$

which appears in a one-body standard Schrödinger equation,

$$\left[-\frac{\hbar^2}{2\mu}\nabla^2+U_{\rm opt}(\boldsymbol{R})+U_{\rm C}(\boldsymbol{R})\right]\chi(\boldsymbol{R})=E_{\rm cm}\chi(\boldsymbol{R})\,. \qquad (13)$$

Here, μ is the reduced mass of the pair, $E_{\rm cm}$ is the center-of-mass energy of the relative motion[18, 19]. $U_{\rm C}(\boldsymbol{R})$ is the Coulomb potential, which can be given as usual by

$$U_{\rm C}(R)=\begin{cases}\dfrac{Z_{\rm P}Z_{\rm T}e^2}{R} & R>R_{\rm C}\\ \dfrac{Z_{\rm P}Z_{\rm T}e^2}{2R_{\rm C}}\left(3-\left(\dfrac{R}{R_{\rm C}}\right)^2\right) & R\leqslant R_{\rm C}\end{cases}, \quad (14)$$

where $Z_{\rm P}$ and $Z_{\rm T}$ are the charge numbers of the projectile and target respectively, $R_{\rm C}=r_0(A_{\rm P}^{1/3}+A_{\rm T}^{1/3})$ is the Coulomb radius of two charged spheres, $r_0=1.2$ fm, $A_{\rm P}$, $A_{\rm T}$ are the mass numbers of the projectile and target, respectively. Eq. (13) is solved in a partial wave expansion and the Noumerov method is adopted for the integration of the radial equation.

In this letter we apply this method to analyze recent experimental data on ^{6}He scattering off ^{12}C at the bombarding energy $E_{\rm lab}=229.8$ MeV at GANIL. ^{6}He is a halo nucleus with a dispersed neutron distribution. We adopt a halo-type density[4], which was obtained by three-body model calculations[20].

$$\begin{aligned}\rho_p(r) &= 2{\rm e}^{-(r/a)^2}/\pi^{3/2}a^3\ ,\\ \rho_n(r) &= 2{\rm e}^{-(r/a)^2}/\pi^{3/2}a^3+\\ &\quad 4({\rm e}^{-(r/b)^2}/3\pi^{3/2}b^5)r^2\ ,\end{aligned} \quad (15)$$

with $a=1.55$ fm, $b=2.24$ fm. A two-parameter Fermi function is used for the density distribution of ^{12}C[4],

$$\rho(r)=\frac{\rho_0}{1+\exp((r-r_0)/a)}\ , \quad (16)$$

with $r_0=2.1545$ fm and $a=0.425$ fm. The density is normalized to the atomic number of ^{12}C, then ρ_0 is determined as 0.207 fm^{-3}. The real and imaginary parts of the optical potential $U_{\rm opt}(R)$ for ^{6}He+^{12}C reaction at 229.8 MeV are calculated by folding the isospin dependent microscopic optical potentials in p(n)+^{12}C with the density of ^{6}He. In our calculations, the radius R_0=15 fm is chosen and the convergence is tested, which is shown in Fig. 1. It is shown that the convergence is easily reached if $m\geqslant 20$. Then $R_0=15$ fm and m=25 are chosen in the following calculations.

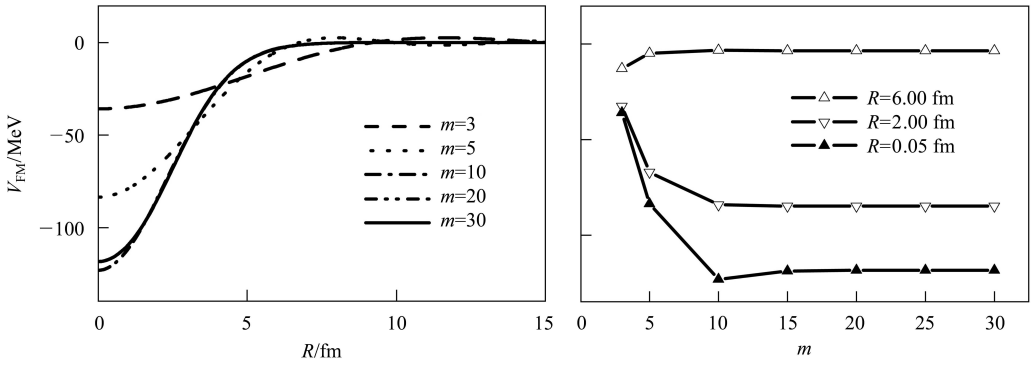

Fig. 1. Test of the convergence in the momentum basis function. The left panel shows the radial distribution of the folded potential with various momentum functions, where only the neutron density in the projectile is included in the calculations. The right panel illustrates the values of the folded potential at $R=0.05$, 2 and 6 fm change with the number of the momentum basis function.

Since ^{6}He is a loosely bound nucleus, a breakup process is one of the main processes in the reaction, which is not considered in the microscopic optical potential of p(n)+^{12}C. The imaginary part of the p(n)+^{12}C optical potential was calculated from the polarization diagram of the $\boldsymbol{G}$-matrix, which takes account of only the processes of particle-hole-type excitations[9]. Thus the calculated imaginary part of the optical potential in the reaction of ^{6}He+^{12}C is much too weak. It is well known that for a weakly bound or halo nucleus its particle threshold is close to the ground state, which implies a strong coupling to the continuum during the interaction of the nucleus with a target. A special treatment of the interaction potential to consider explicitly transitions to the low-lying excited states, to the resonances and breakup states is required, which is usually called the dynamic polarization potential (DPP). In the reaction of ^{6}He+^{12}C, besides the breakup of ^{6}He into the $2n+\alpha$ channel, other complicated processes involving the core breakup will also contribute to the imaginary part of the potential. In order to describe the experimental data of the ^{6}He+^{12}C scattering at $E_{\rm Lab}=229.8$ MeV, one introduces phenomenologically a fac-

tor $N_{\rm I}=3.0$, which is just an enhancing factor of the imaginary part of the optical potential,

$$U_{\rm opt}(R)={\rm Re}V_{\rm FM}(R)+iN_{\rm I}{\rm Im}V_{\rm FM}(R)\,. \qquad (17)$$

The real and imaginary parts of the optical potential in the ^{6}He+^{12}C scattering at $E_{\rm Lab}$ = 229.8 MeV are shown in Fig. 2, where the imaginary part is multiplied by a factor of 3.

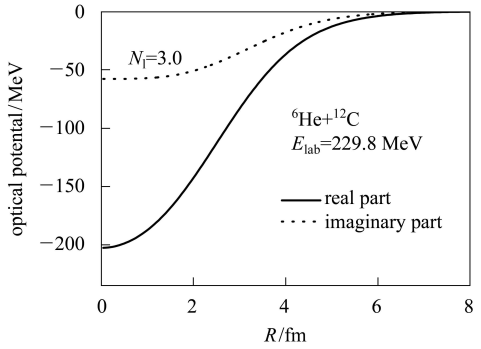

Fig. 2. The real and imaginary parts of the optical potential in the elastic scattering of ^{6}He+^{12}C at 229.8 MeV. The density distributions of ^{12}C and ^{6}He adopted in the calculation are described in the text. The solid and dotted curves represent the real and imaginary potentials, respectively.

3 Discussion and conclusion

The angular distribution in ^{6}He+^{12}C at the bombarding energy $E_{\rm lab}$ = 229.8 MeV is shown in Fig. 3. The differential cross section calculated directly by the folded potential is plotted in Fig. 3 with a dashed curve, which could not reproduce the deep minimum and deviates from the experimental data at the large angles of 10—30 degrees. The solid curve in Fig. 3 corresponds to the result with an enhancing factor 3 in the imaginary part of the folded potential. The agreement between our theoretical calculation and the experimental data is impressive, which is rather encouraging without adjusting more free parameters.

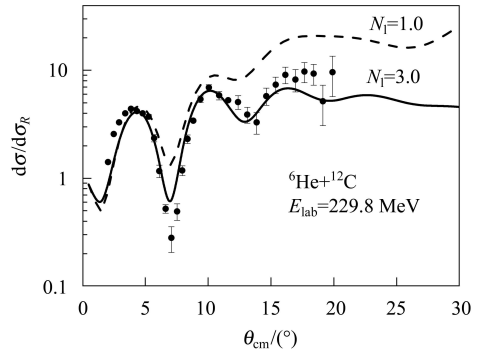

Fig. 3. Angular distribution of the elastic differential cross section for ^{6}He+^{12}C scattering at 229.8 MeV. The solid and dashed curves show the results of the optical model calculations with and without the enhancing factor 3 on the imaginary potential, respectively.

In Fig. 4 we plot the comparison with the results based on various theoretical models. The dotted curve was calculated with a double folding model[4]. In this model the real part of the optical potential was obtained by double folding of the CDM3Y6 effective nucleon-nucleon interaction, and the imaginary part was based on a phenomenological Woods-Saxon type potential with including DPP. In their calculation a best fit to the experimental data was obtained by adding a complex surface potential with a repulsive real part designed to simulate the polarization effects caused by the projectile breakup. The dash-dotted curve corresponds to the calculation in a few-body Glauber model (FBGM)[21], where the ^{6}He wave function is factorized as a three-body wave function consisting of the α core and two neutrons. The target is considered just a scatterer and the effective phases in the Glauber model are calculated from a nucleon-target or a core-target optical potential. It is found that all models could well reproduce the experimental data. At forward angles, our results agree with those of DFM+DPP, while the FBGM produces too deeper minimum. Our results well describe the position of the second minimum in the differential cross section, but value is slightly weak, and so although does FBGM. In general our results are closer to the results of DFM+DPP and the experimental data.

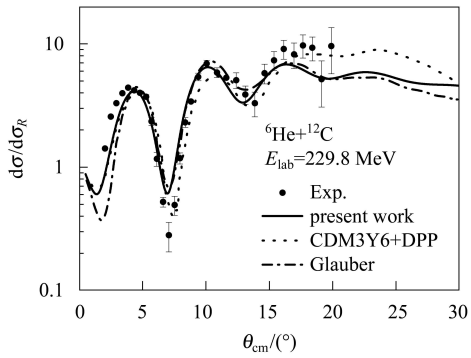

Fig. 4. Same as in Fig. 2 but the dotted, and dot-dashed curves show the results of calculated by the double folding model with CDM3Y + DPP and Glauber model, respectively.

In summary, a microscopic optical model of nucleus-nucleus interaction is first presented with the folding model of nucleon-nucleus optical potential obtained in the framework of the DBHF approach. The

elastic scattering data of ^{6}He at 229.8 MeV on a ^{12}C target have been analyzed within the standard optical model. A factor of 3 on the imaginary potential to take account of phenomenologically the breakup and complicated processes is introduced. The calculated ^{6}He+^{12}C elastic scattering differential cross section is in good agreement with the experimental data. A comparison with the DFM+DPP based on the M3Y interaction (CDM3Y6) and the FBGM is presented. Our results could be potentially important for the description of composite particles scattering of many-body systems and unstable nucleus-nucleus systems, especially. Naturally, a further test of our model will be desired. A more detailed account of our work will include extensive comparison with the elastic scattering data of several other heavy ion systems, which will be reported in a forthcoming paper.

References

1 Satchler G R, Love W G. Phys. Rep., 1979, **55**: 183
2 Furumoto T, Sakuragi Y. Phys. Rev. C, 2006, **74**: 034606
3 Bertsch G, Borysowicz J, McManus H et al. Nucl. Phys. A, 1977, **284**: 399
4 Lapoux V, Alamanos N, Auger F et al. Phys. Rev. C, 2002, **66**: 034608
5 Chamon L C, Pereira D, Hussein M S et al. Phys. Rev. Lett., 1997, **79**: 5218
6 Alvarez M A G, Chamon L C, Hussein M S et al. Nucl. Phys. A, 2003, **723**: 93
7 Khoa Dao T. Phys. Rev. C, 2001, **63**: 034007
8 XU C, REN Z Z. Phys. Rev. C, 2006, **74**: 014304
9 RONG J, MA Z Y, Giai N V. Phys. Rev. C, 2006, **73**: 014614
10 Schiller E, Müther H. Eur. Phys. J. A, 2001, **11**: 15
11 MA Z Y, CHEN B Q. J. Phys. G: Nucl. Part. Phys., 1992, **18**: 1543
12 Bell J S, Squires E J. Phys. Rev. Lett., 1959, **3**: 96
13 Horowitz C J, Serot B D. Nucl. Phys. A, 1981, **368**: 503
14 Horowitz C J. Nucl. Phys. A, 1984, **412**: 228
15 Horowitz C J, Serot B D. Nucl. Phys. A, 1987, **464**: 613
16 Jaminon M, Mahaux C, Rochus P. Phys. Rev. C, 1980, **22**: 2027
17 Petrovich F. Nucl. Phys. A, 1975, **251**: 143
18 MA Y Q, MA Z Y. Acta Phys. Sin., 2008, **57**: 74 (in Chinese)
19 MA Y Q, ZOU W, MA Z Y. J. Phys. G: Nucl. Part. Phys., 2008, **35**: 065108
20 Al-Khalili J S, Tostevin J A, Thompson I J. Phys. Rev. C, 1996, **54**: 1843
21 Abu-Ibrahim B, Suzuki Y. Nucl. Phys. A, 2003, **728**: 118